INTERNATIONAL ATOMIC ENERGY AGENCY
UNITED NATIONS EDUCATIONAL, SCIENTIFIC AND CULTURAL ORGANIZATION

INTERNATIONAL CENTRE FOR THEORETICAL PHYSICS
34100 TRIESTE (ITALY) - P.O.B. 586 - MIRAMARE - STRADA COSTIERA 11 - TELEPHONES: 224281/2/3/4/5/6
CABLE: CENTRATOM - TELEX 460392-1

SMR/113 - 10

AUTUMN COLLEGE

ON

THE TROPOSPHERE, STRATOSPHERE AND MESOSPHERE

10 September - 19 October 1984

MEASURING TECHNIQUES AND MEASUREMENTS :

GROUND-BASED, LIDAR AND ROCKETS

L. THOMAS

Department of Physics
University College of Wales
Aberystwyth SY23 3BZ
Wales
U.K.

Classification of Atmospheric Regions

Many different types of atmospheric features can be measured: thermal structure, dynamical parameters, concentrations of major constituents (e.g. O_2, N_2, CO_2), concentrations of minor constituents (e.g. H_2O, O_3, NO_2), visible phenomena (clouds, aurorae) or electric change (electrons or ions).

However, a central part in studies of atmospheric physics is the transformation of energy which takes place, and the dynamical and thermal structures of the atmosphere represent the best indicators of such transformations. Dynamical factors, such as wind, are far too variable to be of use in general discussion and it is, therefore, customary to classify the atmospheric regions on the basis of thermal structure.

Near the ground, the temperature decreases with increasing height at a rate of about 6.5^{o} per km, in the troposphere, and above this region there is a complicated structure with regions separated by 'pauses'. The troposphere is influenced by conditions near the Earth's surface and induced circulation; the stratosphere is controlled by absorption of certain parts of the solar spectrum, chiefly uV , in ozone and convection; in the mesosphere a larger part of the solar spectrum is available and photochemistry is important.

Composition

Up to about 100 km - the turbopause - the atmosphere is known as the homopause in that the main constituents remain completely mixed and consequently the mean molecular weight is constant.

However, a very complicated neutral composition exists which can for convenience be considered in terms of families of constituents - meteorological gases (O_3, H_2O, CO_2), chlorine compounds, nitrogen oxides, etc.

In addition, solar radiation capable of ionizing atmospheric gases can penetrate down to about 70 km and galactic cosmic rays are responsible for producing ionization at still lower heights, down to ground level.

Pressure (mb)	Number density (cm^{-3})	Mean free path (cm)	Mean molecular weight
1.64(-3)	6.57(13)	2.6	28.96
5.52(-2)	1.82(15)	9.3(-4)	28.96
7.93(-1)	2.14(16)	7.9(-3)	28.96
1.20(1)	3.30(17)	4.4(-4)	28.96
2.7(2)	8.6(18)	2.0(-5)	28.96

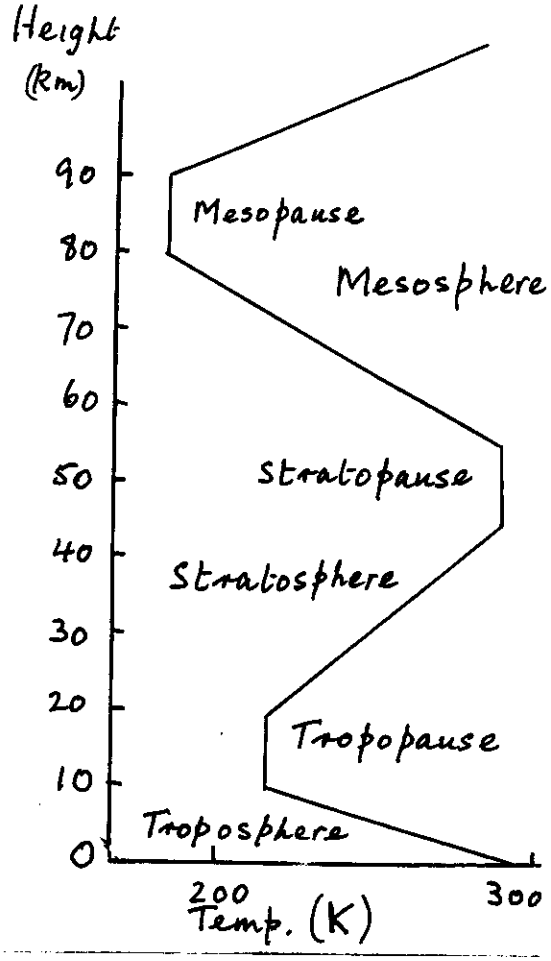

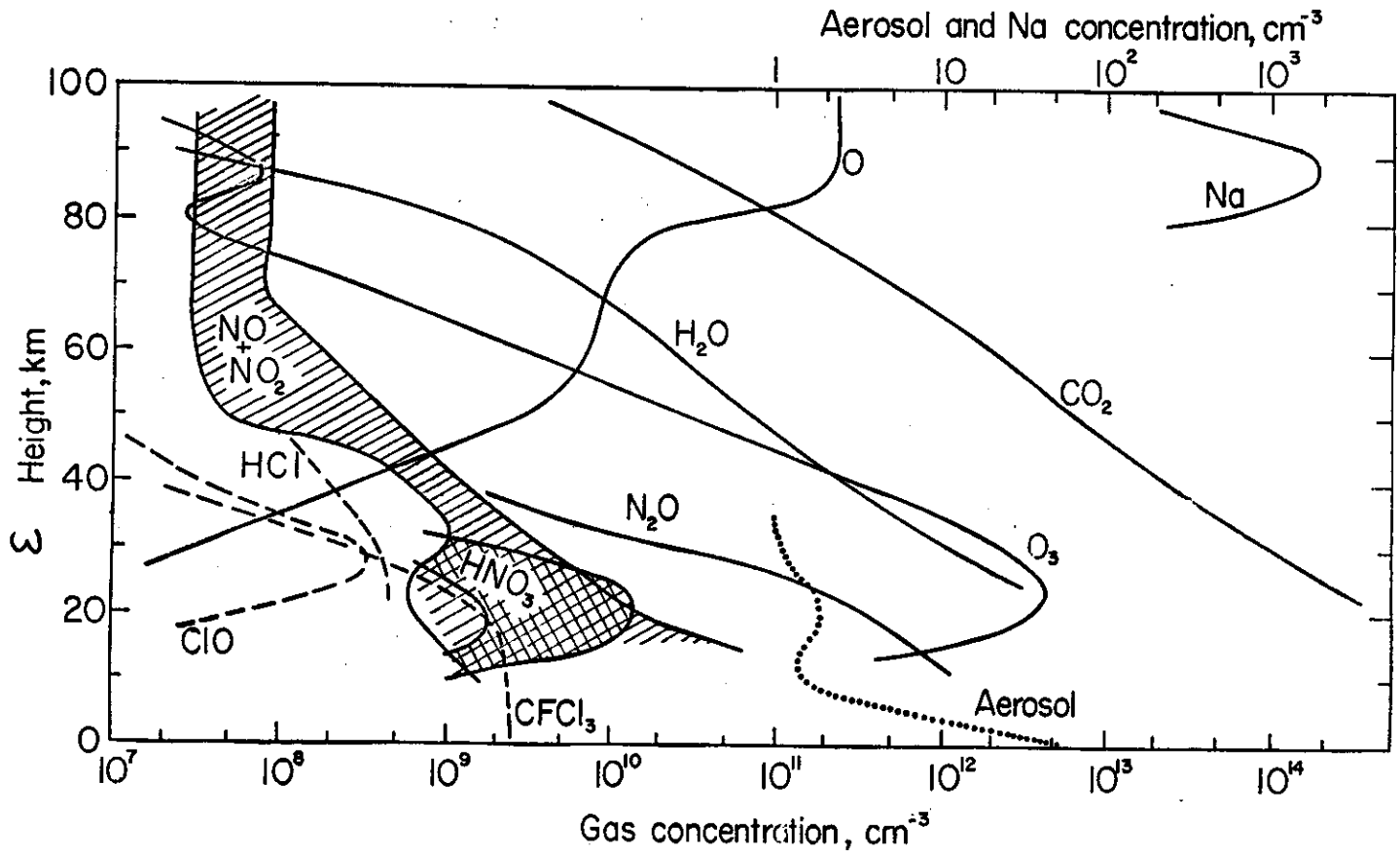

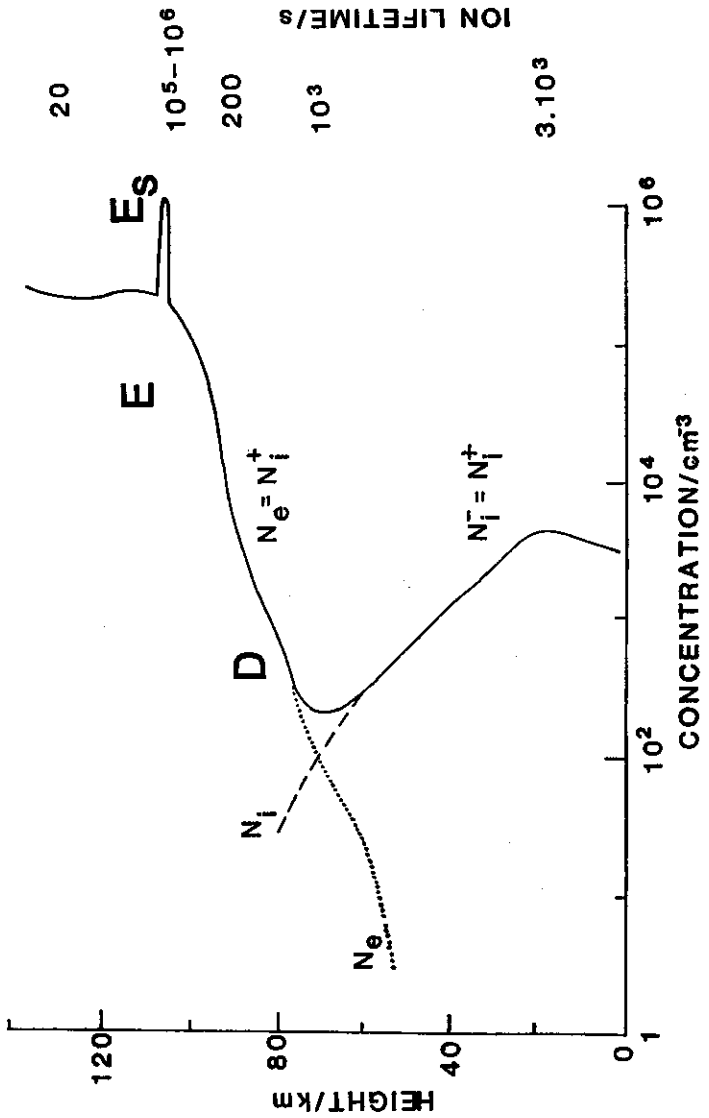

4

Interelations between pressure (p), temperatures (T) and density (ρ)

Air is approximately in hydrostatic equilibrium

$$\frac{dp}{dh} = -g\rho$$

The equation of state:

$$p = \rho \frac{RT}{m}$$

where R represents universal gas constant and m the mean molecular weight.

From there it can be shown that for an isothermal atmosphere

$$p = p_o \exp\left(-\frac{mg}{RT} \cdot h\right) = p_o \exp\left(-\frac{h}{H}\right)$$

where p_o corresponds to h = o and H is a characteristic length, known as the scale height.

In addition

$$n = n_o \exp\left(-\frac{h}{H}\right)$$

Footnote

In troposphere, m the mean molecular weight includes a contribution from water vapour and if a distinction is to be drawn with dry air

$$p = \rho \frac{RT}{m} = \rho \frac{R}{m_{dry}} \left(\frac{1 + w/\epsilon}{1 + w}\right)$$

where w = $\frac{\text{density of vapour}}{\text{density dry air}}$ and $\epsilon = \frac{m_{vap}}{m_{dry}}$

5

In the presence of a fixed gradient of scale height

i.e. $H = H_0 + \beta h$

better approximations are given by

$$p = p_0\left(\frac{H}{H_0}\right)^{-\frac{1}{\beta}}$$

$$n = n_0\left(\frac{H}{H_0}\right)^{-\left(\frac{1+\beta}{\beta}\right)}$$

Measurements of pressure, temperature and density

For the troposphere, and particularly with the aim of giving synoptic charts at fixed pressure levels, instrumented balloon (radiosondes) are used at a network of sites. The height limit is about 30 km (10 mb) at which the balloon bursts. Devices for measuring pressures at tropospheric and stratospheric heights are included as well as humidity and temperature sensors. These will be discussed in the lecture series given by Dr. Barnett.

The Meteorological Rocket Network was set up in 1959 to examine more closely some of the features of the stratospheric circulation indicated in balloon studies. However, the use of rockets for atmospheric studies had been initiated after the war, initially with Nike Cajun and Nike Apache rockets, and subsequently Arcos, Lokte and Petrel types.

The type of techniques used in the rocket measurements of atmospheric structure will be outlined, one or two types being considered in some detail, and examples of intercomparisons given to illustrate their relative merits.

Although measurements of temperature are made directly, as with the bead thermister approach, or inferred directly from the primary measurements, such as that of the velocity of sound, several of the temperature data have been deduced from measurements of pressure or density.

The principles of three of the most commonly used techniques are given below:

(a) Falling sphere experiment

This makes use of the acceleration of a freely falling sphere ejected from a rocket near the highest part of its flight. The effects of air motion are assumed to be small and the principal forces are those due to gravity and an upward force due to the drag of the surrounding air. The acceleration due to this force is given by

$$a = \frac{\rho V^2}{2M} A C_D$$

where

ρ = atmospheric density

V = velocity of fall

A = cross-sectional area

M = mass

C_D = drag coefficient, which is a function of V and Reynolds number.

Solving for ρ and integrating hydrostatic equation, obtain for pressures

$$p_2 - p_1 = \int_{h_2}^{h_1} g\rho\,dh$$

and using equation of state,

$$T_2 = \frac{\int_{h_2}^{h_1} g\rho\,dh}{\rho_2 R} + \left(\frac{\rho_1}{\rho_2}\right) T_1$$

A knowledge of T_1, at an upper reference level, is required but if ρ_1/ρ_2 is small, the error in T_2 is small. The details and performance of the two forms of this experiment are given later

(b) Pitot tube

The measurement of the impact pressure (p_1) at a suitably designed nose, together with that of the ambient pressure (p_a), gives ρ from Rayleigh's pitot tube theory

$$\rho = \frac{a p_1 - b p_a}{V^2}$$

where a and b are constants, depending on units adopted.

From a knowledge of p and ρ, T can be found.

The pressure sensor normally used is a radioactive ionization gauge.

(c) Rocket grenade experiment

This measurement of temperature depends on the measurement of the velocity of sound $c \left(= \left(\frac{\gamma RT}{m}\right)^{\frac{1}{2}}\right)$. The method makes of a series of grenades ejected from rockets, the times of travel of sound to the ground being measured.

With the geometry being known, a measurement of t_1 and t_2 enables the wind V_{12} to be deduced and also the time taken for sound to travel between the two levels.

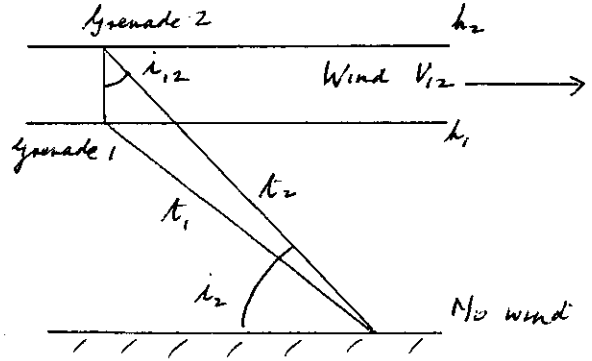

Then by assuming there is no wind at the ground, the application of Snell's law gives

$$\frac{c_{12} + V_{12}}{\sin i_{12}} = \frac{c_0}{\sin i_2}$$

Also

$$c_{12} \cos i_{12} = \frac{h_2 - h_1}{t_{12}}$$

and from these relations C_{12} and, therefore, T_{12} can be deduced.

Details of falling sphere experiments

7 inch small rigid falling sphere

An accelerometer inside the sphere measures accurately the drag acceleration, the data being telemetered to the ground. The measurement is made in terms of the time of fall of a reference mass, a value as low as 5×10^{-5} g being measurable.

The reference mass is a 1 inch spherical bobbin surrounded by a spherical cavity, the diameter of the two differing by 0.12 inch. The impact of the bobbin with the spherical cavity is monitored electrically. The bobbin is centred in the cavity by pins driven by hydraulically operated activators, the mechanical forces being supplied by electromagnetic drive units. Corresponding to the release of the bobbin from the centre position and its arrival at the cavity, pulses of 10 μs and 20 μs are generated. These are then used to amplitude modulate the telemetry and the time interval between the two pulses gives the sphere fall time. The method can be used over the height range 30-140 km.

Inflatable passive sphere

Ground-based radar are used to track a metalised one-metre mylar sphere. The folded form of this sphere is ejected from a canister by an expansion charge with rapid inflation being accomplished by the vapourisation of isopentane liquid.

Below 30 km the sphere tends to collapse due to the ambient pressure being greater than the internal vapour pressure. For heights above 90 km the drag force is too small to be measurable.

Comparison of measurements made with these two falling sphere experiments and with the pitot tube and thermistor bead sensor will be given to demonstrate the performance of these devices.

10

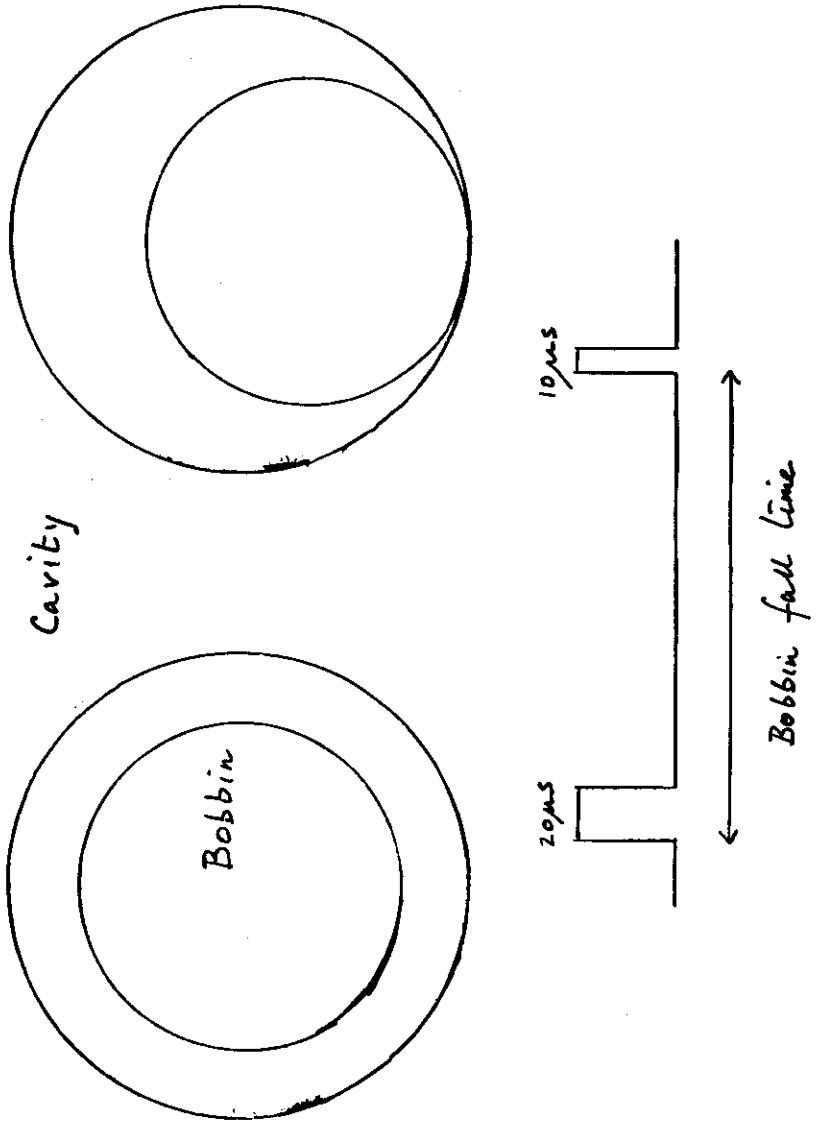

11

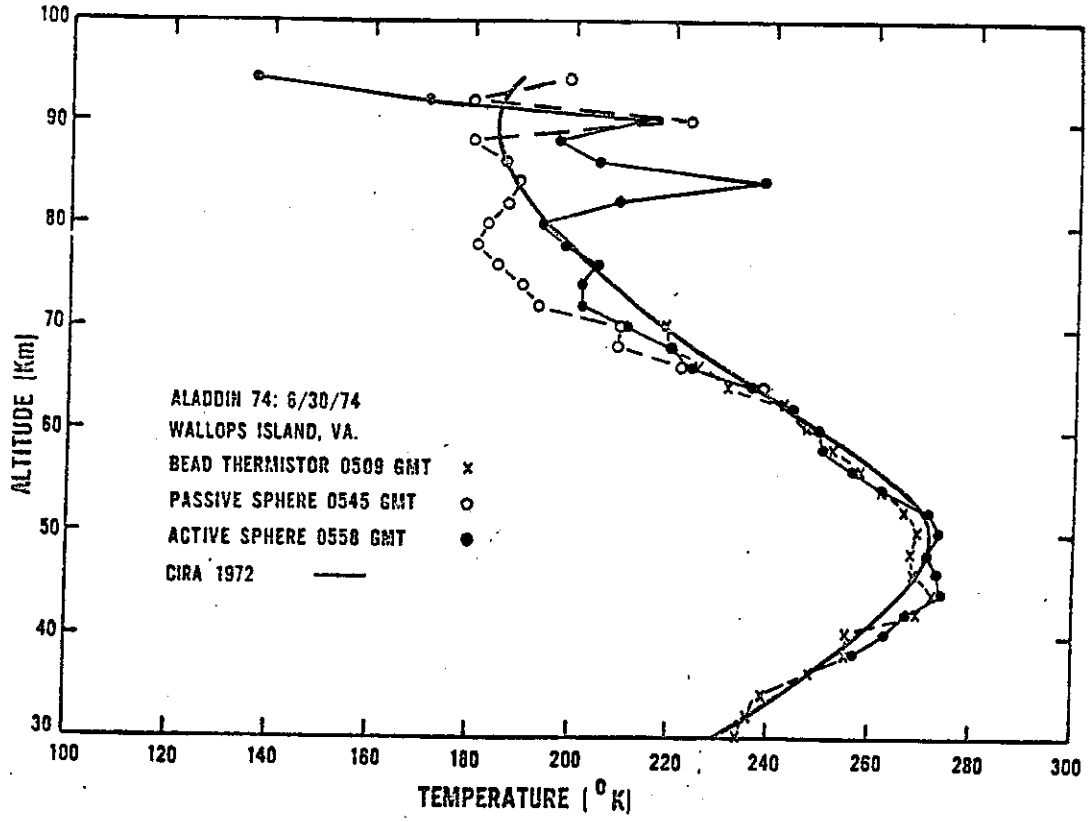

Figure 1

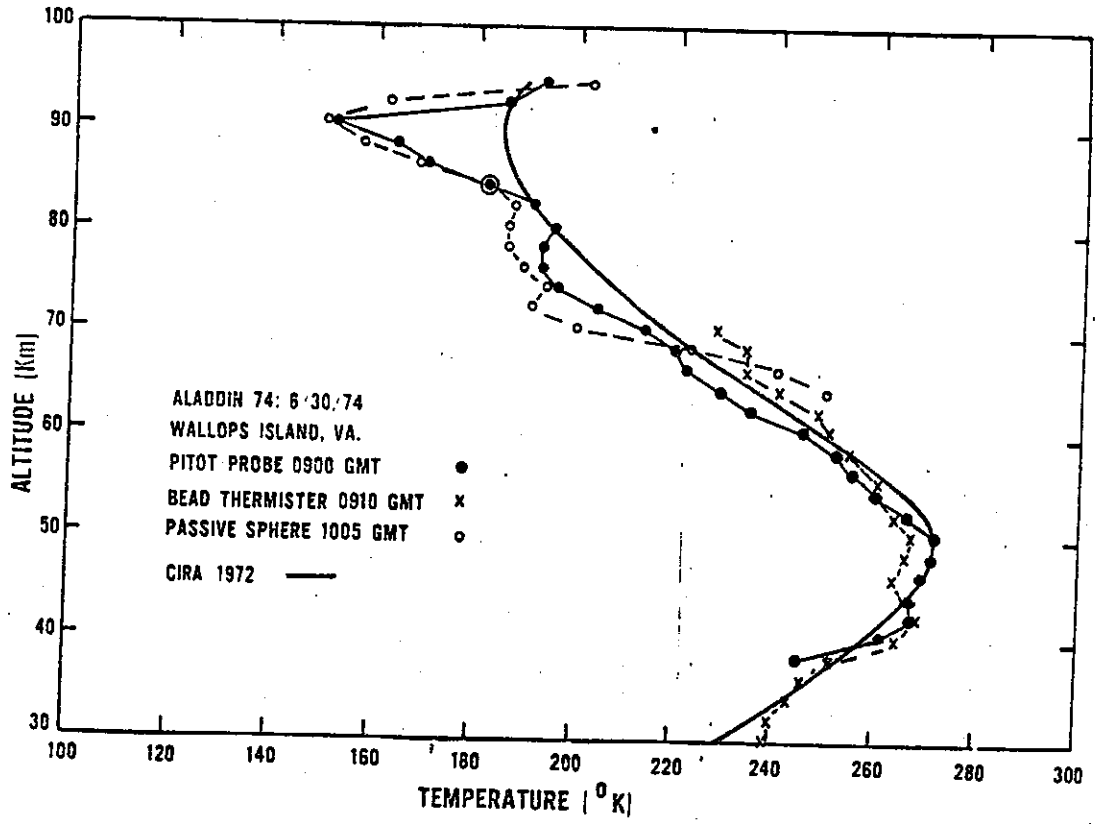

Figure 3

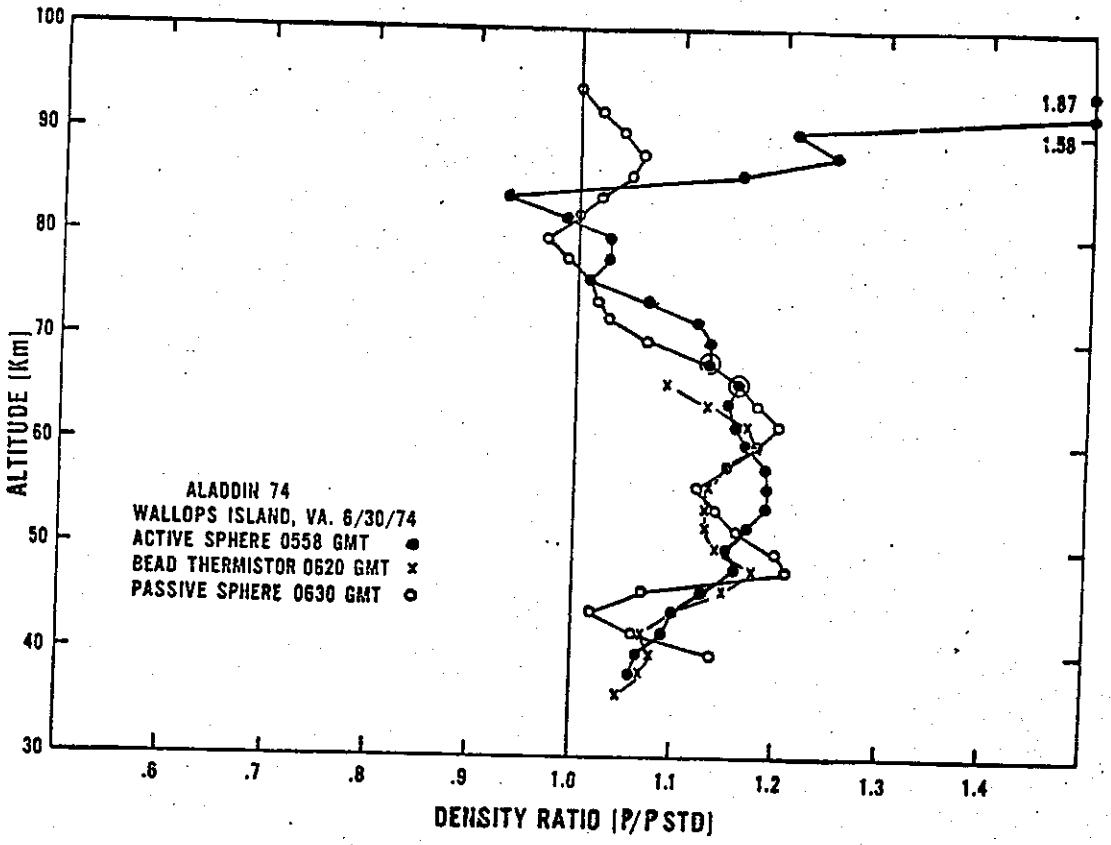

Figure 4

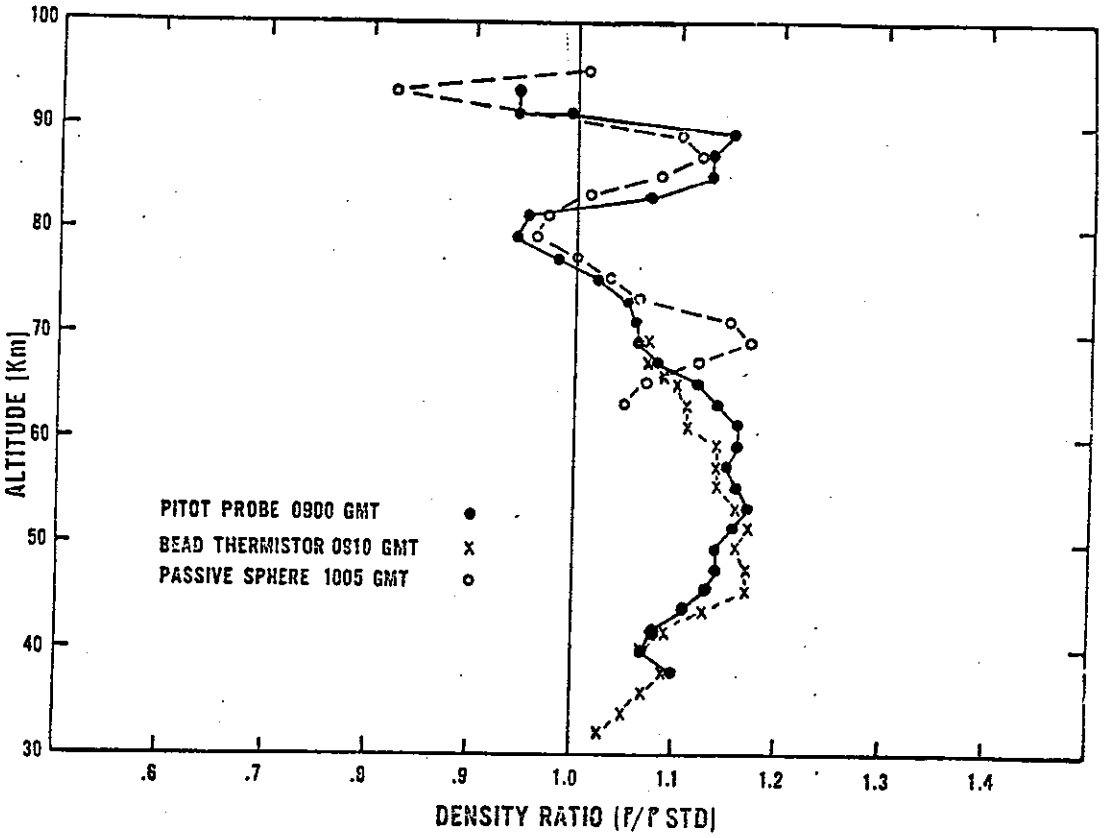

Figure 5

Mass-spectrometer experiments

Mass-spectrometer measurements have chiefly related to the ion composition but with the incorporation of suitable ionizing sources they can also be applied to neutral constituents.

Below 90 km, the mean free path of ions becomes comparable with the path length of ions within the spectrometer, thus interfering with the performance of the instrument. Arrangements for pumping to low pressures need to be incorporated in the experiment. For most measurments at these heights, quadrupole mass spectrometers with cryogenically cooled pumping systems have been employed.

Instrument operation is based on mass analysing properties of linear quadrupole electric fields. For potentials of $\pm (U + V\cos\omega t)$ applied to opposite pairs of electrodes of hyperbolic shape, potential at point (x, y) is given by

$$\phi(x,y) = \left(\frac{x^2 - y^2}{r_0^2}\right)(U + V\cos\omega t)$$

This has feature that x and y components of electric field are independent of y and x respectively, so that ions have independent velocities in x and y directions.

Equation of motion of ion has two possible solutions

1. Motion in Z direction with constant velocity and exponentially increasing amplitude of oscillations in x and y directions; ions lost to electrodes.

2. Motion in Z direction with constant velocity but with stable orbiting paths; ions pass through electrode system to collecting plate.

Solution 2 is possible if ratio $\frac{U}{V} \geq 0.166$ and for this value the mass to charge ratio is determined by $V/r_0^2\omega$. Mass analysis affected by changing U and V with time, keeping ratio constant, the mass range being determined by and range over which V is varied.

Details of one experimental system will be described.

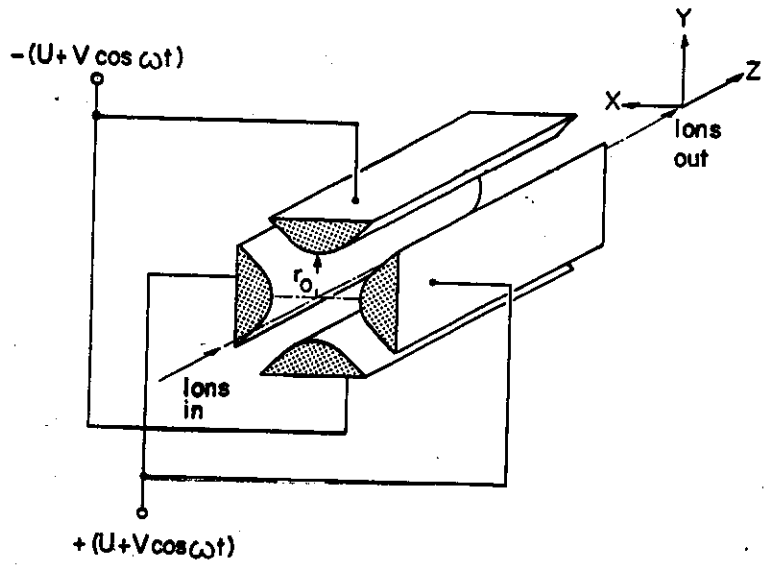

Fig. 32

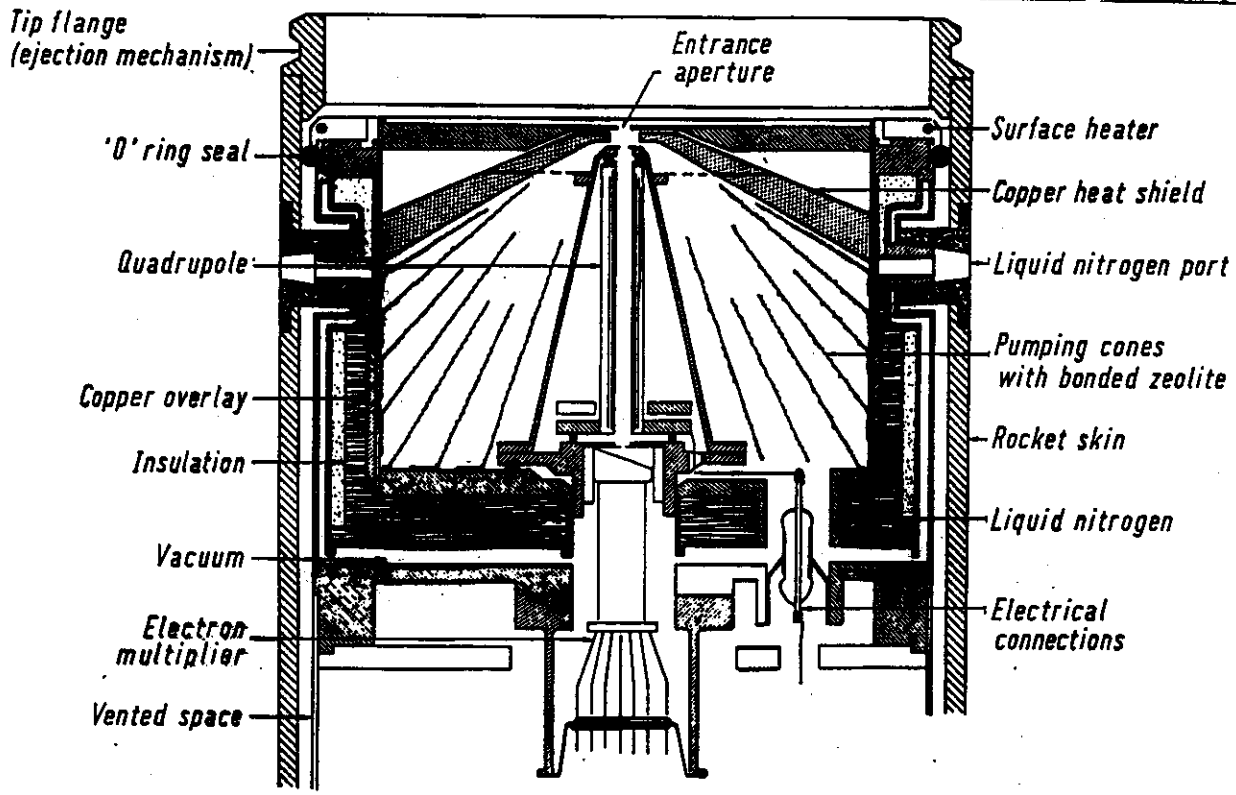

A cross-sectional view of the quadupole mass spectrometer system with liquid-nitrogen cooled zeolite adsorption pump, after NARCISI and ROTH[19]

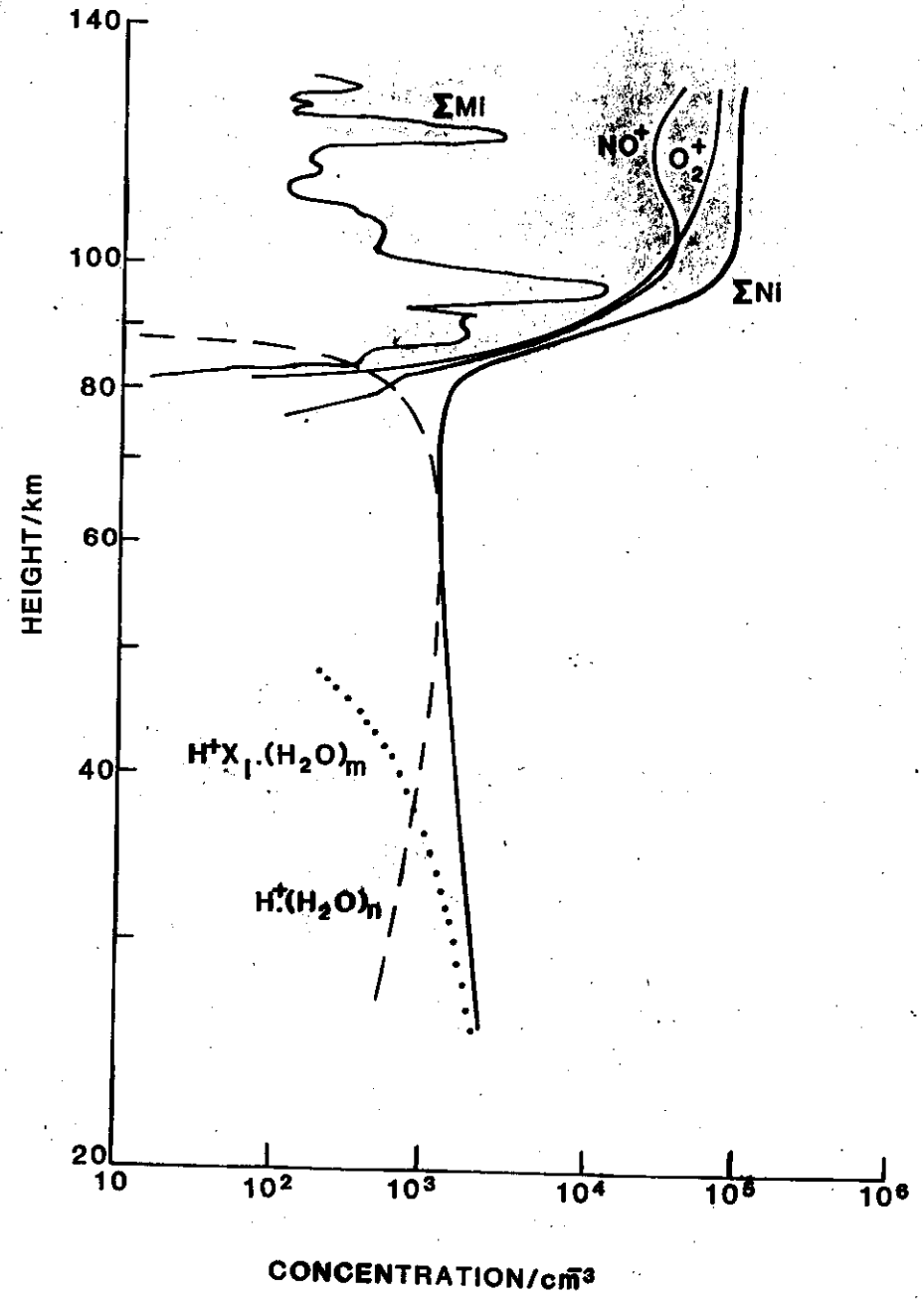
140
100
80
60
40
20
ΣMI
NO+
O2+
ΣNi
H+X1.(H2O)m
H+(H2O)n
HEIGHT/km
10
10²
10³
10⁴
10⁵
10⁶
CONCENTRATION/cm⁻³

20

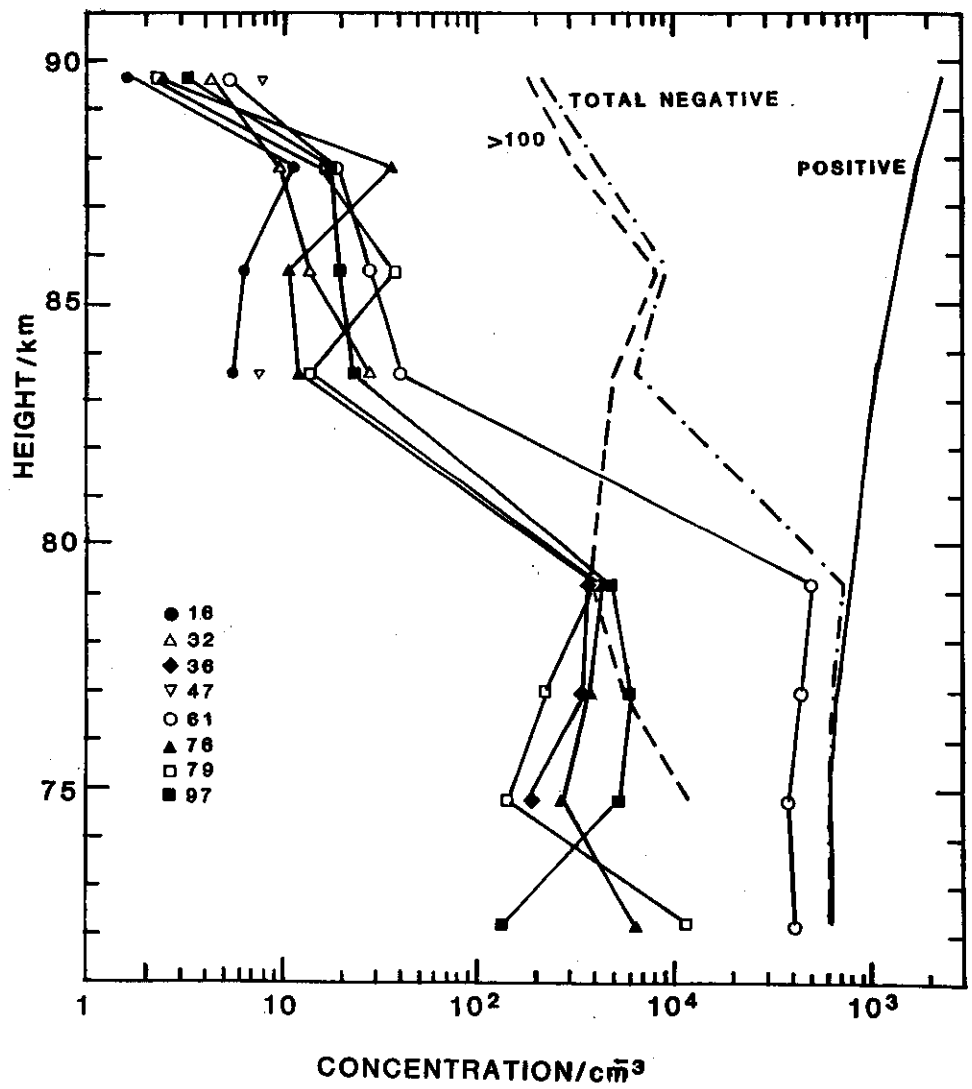
90
85
80
75
TOTAL NEGATIVE
>100
POSITIVE
16
32
36
47
61
76
79
97
HEIGHT/km
1
10
10²
10⁴
10³
CONCENTRATION/cm⁻³

21

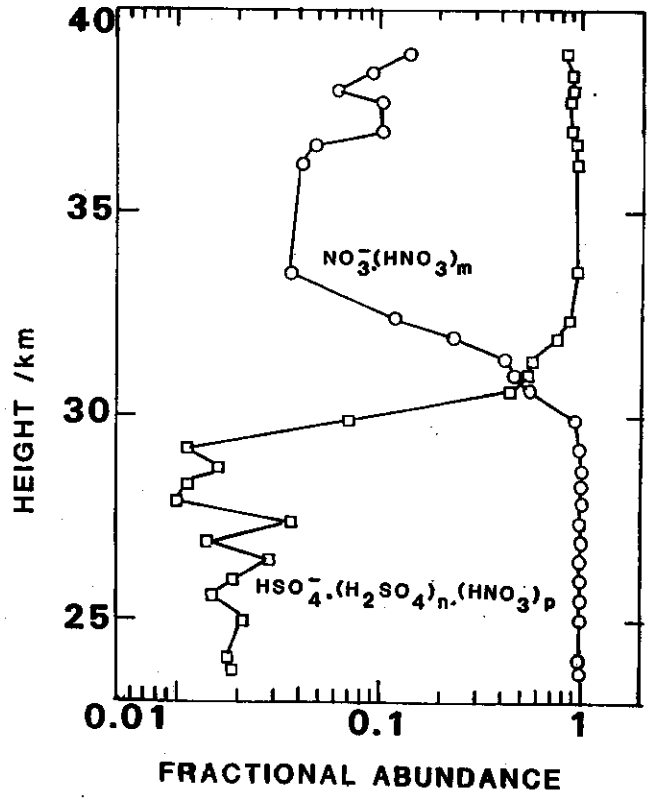

Lidar measurements of atmospheric parameters and constituents

Lidar, light detection and ranging, depends on the interaction of laser radiation with individual molecules or particles, followed by scattering or re-radiation. The interaction depends on the size of the molecule or particle in relation to wavelength and the specific state of the molecule, i.e. energy state, pressure, temperature. The lidar technique has been used for remote sounding of the troposphere, stratosphere and mesosphere.

The second type of interaction arises from fluctuations in refractive index caused by turbulent structure of the atmosphere and is of particular interest in the lower atmosphere.

Although optical radar was initiated with searchlights, its exploitation followed the development of pulsed lasers since the monochromatic nature of these sources allows the use of narrow-band filters to discriminate against background light. Also because the beams are virtually monochromatic and highly coherent they can be well collimated (beam widths of 1 m rad are normal) and this also minimises background light interference.
The method involves a transmitter and perhaps collimater arrangement, the radiation scattered by the atmosphere being received on a fairly large concave mirror normally greater than 30 cm diameter. It is then passed to a photomultiplier and then to a recording system, normally triggered by part of the laser beam (perhaps generating a voltage pulse in a photodiode) and thereby providing a measurement of the range of the atmospheric scattering volume.

The radar equation for vertical incidence then gives the number of photodetectors generated by a laser pulse scattered from a height interval δh at a height h with no change of wavelength:

$$C = N_t \frac{T^2 A \sum_i (\sigma_i n_i) \delta h}{h^2} \eta$$

where N_t = number of photons leaving the transmitter optics per pulse

T = the atmospheric transmission up to h

σ_i = the differential back scattering cross section

n_i = number density of scatterers at height

A = receiver mirror area

η = overall receiver optical efficiency

As an example, a Ruby laser of about 1J per pulse scattered from O_2 or N_2 near 50 km give rise to 1 or 2 photoelectrons per laser firing. The exploitation of the laser then depends on the different values of n_i and σ_i for gases or aerosols (particles) which are turbulently mixed in the atmosphere.

Before considering the type of application of lidar systems, we should be familiar with the variety of interactions with molecular or particles that are possible for optical wavelengths.

Summary of Scattering Processes

Elastic

1. Scattering from aerosols (particles) forms an important contribution to signals returned from heights below 30 km.
   Particles sizes are substantially greater than the sounding wavelengths, ranging in radii from 10^{-7} mm to 10^{-1} mm.

$$\sigma \sim 10^{-31} \text{ to } 10^{-12}\ m^2 sr^{-1}$$

2. Rayleight scattering

   From molecules when wavelength does not coincide with absorption time and particles much smaller than wavelength

$$\sigma \propto \lambda^{-4}\left(1+\cos^2\theta\right)$$

where θ is scattering angle.

for visible radiation, $\sigma \sim 10^{-31}\ m^2 sr^{-1}$

3. Resonant or fluorescent scattering.
   Occurs when frequency corresponds to absorption line or band.
When scattered radiation at incident frequency - resonant.
When scattered radiation at lower frequency than incident - fluorescent

$$\sigma \lesssim 10^{-16}\ m^2 sr^{-1}$$

Inelastic

Raman scattering.

A significant exchange of energy occurs between the photon and the scattering medium, the Raman scattered component being shifted from the incident frequency by an amount corresponding to the internal energy of the species.

For rotational Raman, cross section two orders of magnitude larger than for vibrational-rotational case, which is itself about 3 orders of magnitude smaller than that for Rayleigh scattering.

Choice of lasers

Clearly depends on the specific objectives of the measurements but in general attention needs to be paid to both the scattering and absorption of the laser beam. The relative importance of these two components can be considered for lasers at operating wavelengths from the ultraviolet to infra-red, with particular attention to the λ^{-4} dependence for Rayleigh scattering and the possibility of selective absorption of certain wavelengths by particular gaseous constituents.

For wavelengths in excess of about 3 μm the technique depends on returns from aerosols.

The greater scattering efficiency at uv or visible wavelengths would favour sources operating at these wavelengths but the choice is complicated by the greater efficiency of ir lasers, e.g. CO_2 at 10.6 μm, and coherent detection at these longer wavelengths offers a substantial improvement.

In the uv or visible region, the most convenient sources are Ruby or Neodymium-Yag,with arrangements for frequency doubling. However, since these depend on transactions between specific energy levels they are restricted to certain wavelengths. If a wider wavelength range is required, the vibrational-rotational transitions possible with an organic dye provides a laser with an operating spectral range of about 5-10 nm; dispersive elements, such as a Fabry Perot etalons or diffraction gratings within the laser cavity then provide wavelength selection.

Lidar system parameters

Clearly depend on the particular application of the experiment and the sensitivity required. Thus for receiving, simple mirrors of spherical or parabolic shape and diameters of 30 cm or less have been commonly used but one system made use of a complicated mosaic construction of 36 mirrors each of 75 cm diameter.

The design of system needs to take account of the range envisaged, and the sensitivity with reference to background noise, system noise and dynamic range. The receiver beamwidth and narrow-band filters are chosen to minimise background light from the sky. For observation of Rayleigh scattering over range of troposphere, stratosphere and mesosphere, the receiver should be capable of amplitude change by 10^6. However, for a single photomultiplier a dynamic range of about 20:1 is typical and for any sizeable range of heights more than one unit is required.

Types of lidar measurements

1. Optical transmission of atmosphere.
2. The distribution of aerosols.
3. Some characteristics of ice crystals in cirrus clouds.
4. Atmospheric constituents:
   (a) by Raman scattering
   (b) by differential absorption
   (c) by resonant and fluorescent scattering.

Future developments

Wealth of spectral features of atmospheric constituents in the near infra-red favour the use of CO_2, CO and HF laser for composition studies. However, heterodyne detection is necessary.

Measurement of wind velocities using aerosols as tracer, with either narrow band, stable visible laser or coherent CO_2 laser with heterodyne detection.

The exploitation of lidar experiments operating downwards from the space shuttle to provide both world-wide coverage and very good height resolution.

$T = \exp(-\gamma \Delta L)$

$= \exp(-\tau)$

τ = optical depth

Absorption $K = K_m + K_a$

Scattering $S = S_m + S_a$

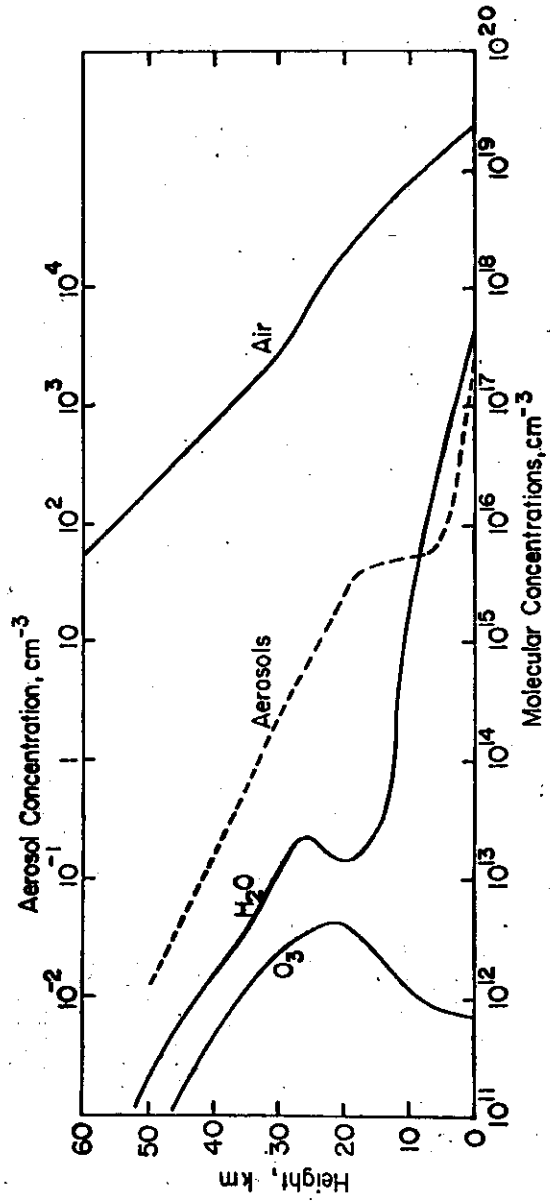

Fig. 6 Height Distributions of Molecules and Aerosols

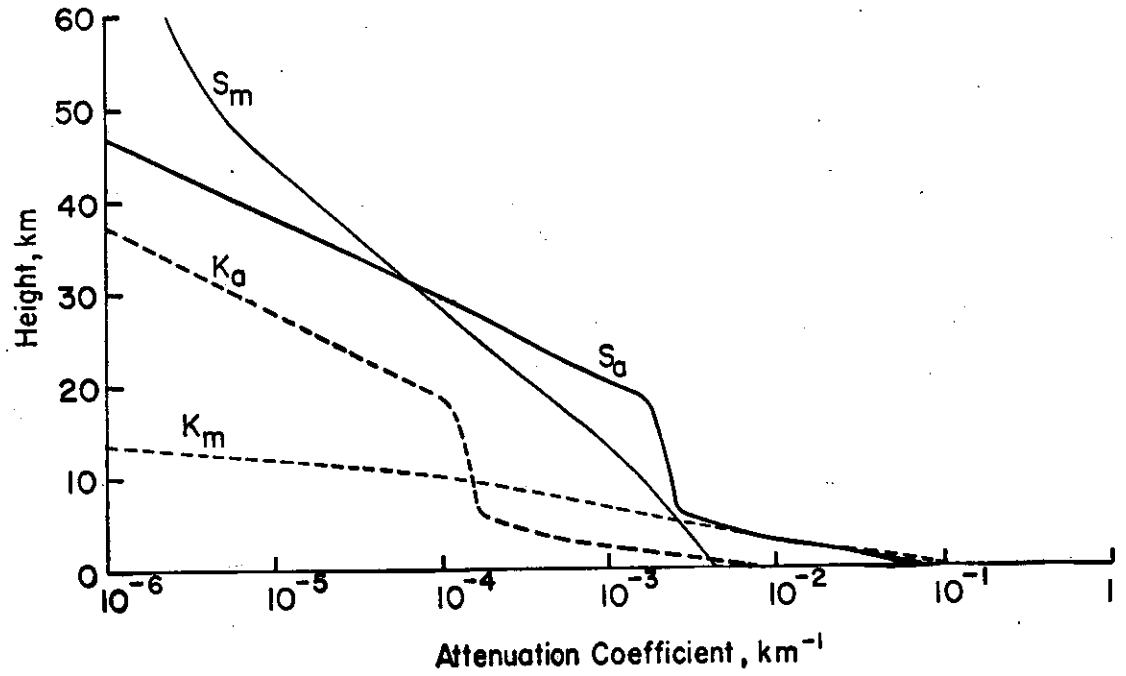

30

Molecular and Aerosol Absorption and Scattering
for Ruby Laser Wavelength (0·6943 μm)

RSRS REF NO 1889/2

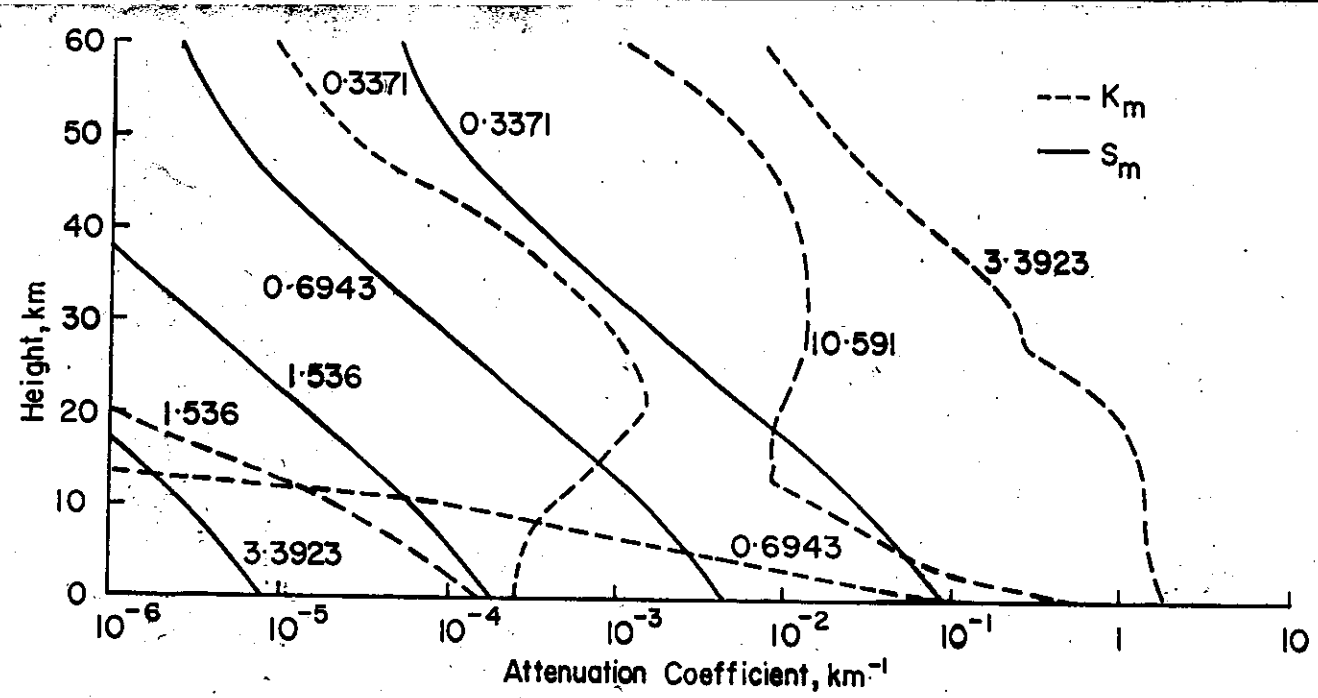

31

Molecular Absorption and Scattering for Different Laser Wavelengths (μm)

RSRS. REF. No. 1889/1

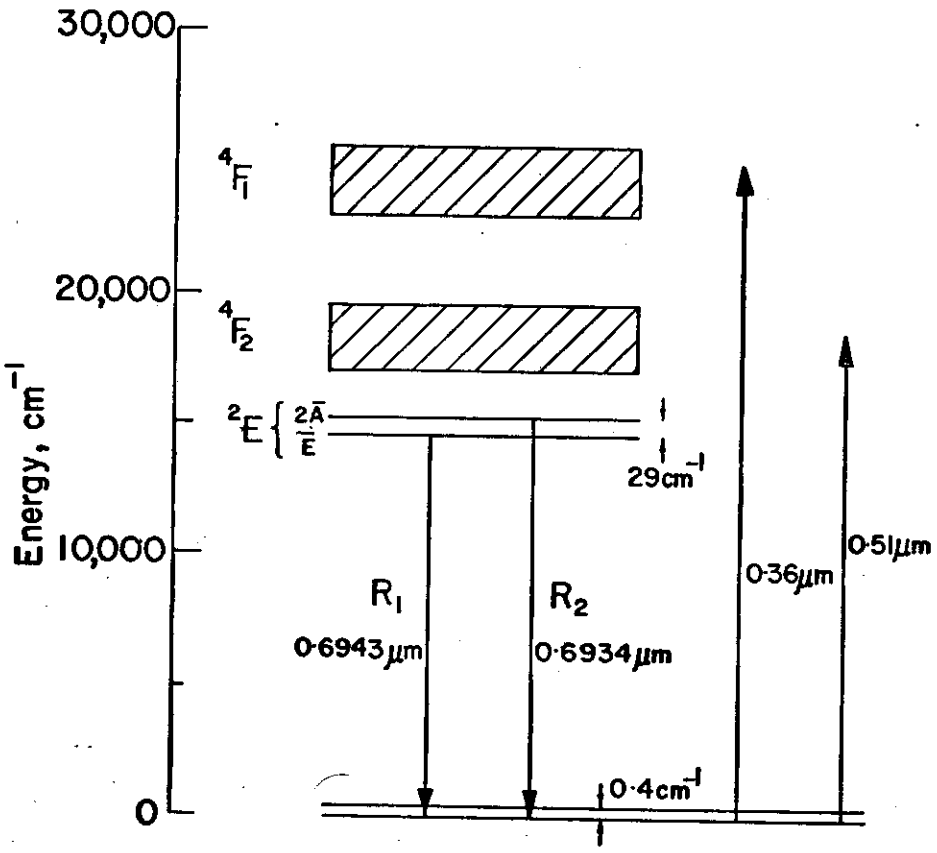

Energy of Chromium Ion in Ruby

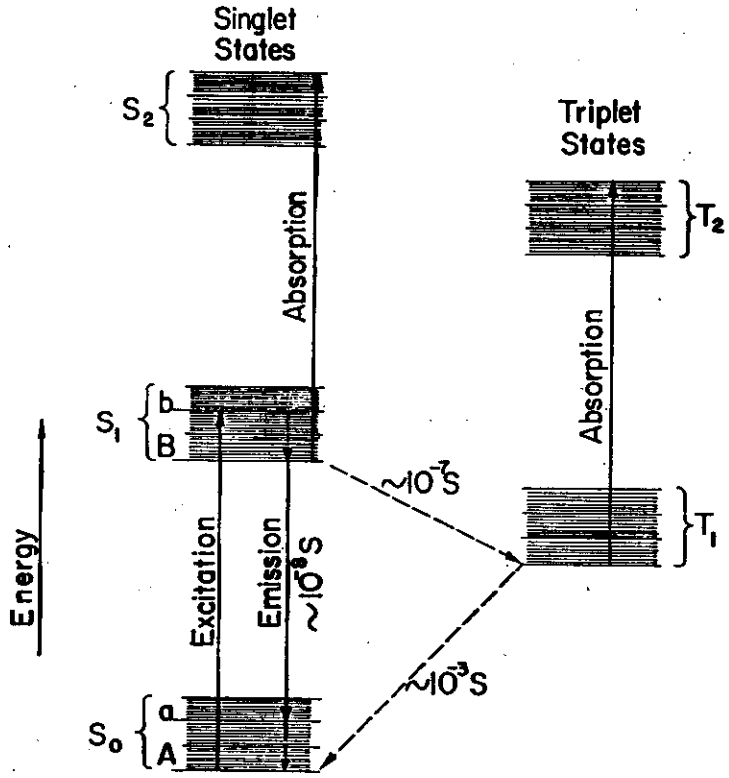

Energy Levels of a Dye Molecule

RSRS REF No 1889/8

34

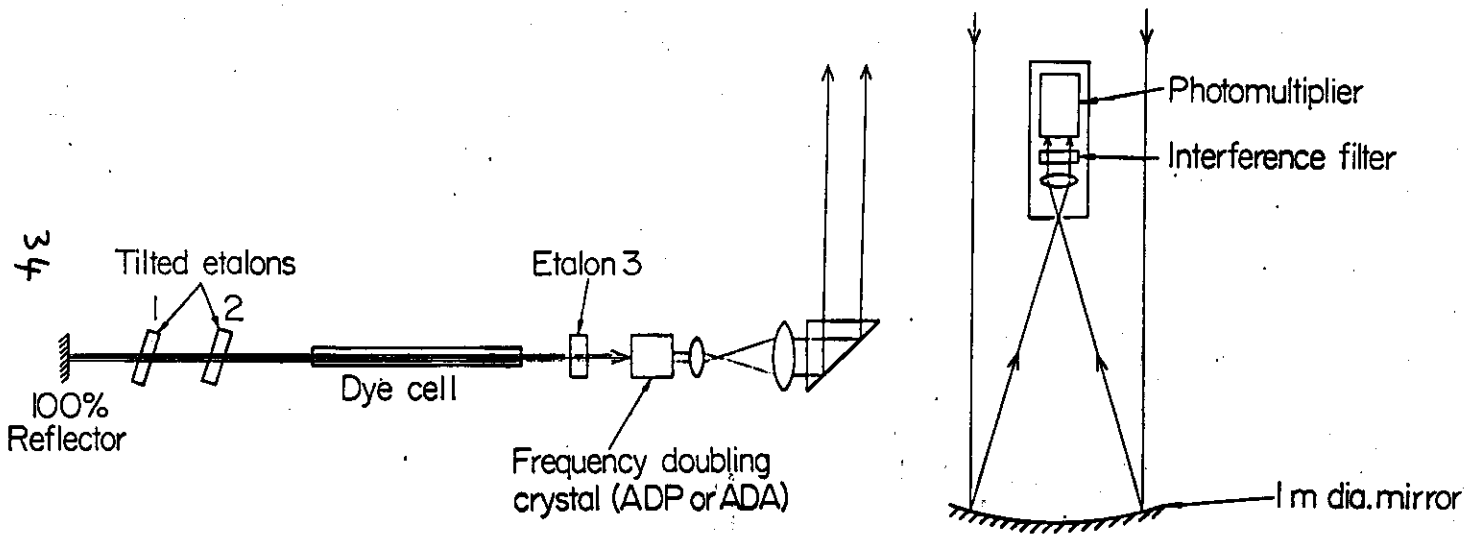

35

$$c = \frac{N_t \sin\alpha\, r^2 \operatorname{cosec}\alpha\, \Delta\eta\, \Sigma_1(\sigma_1 n_1)\, \delta R}{\text{[illegible]}^2}$$

$$\therefore \log c = 2 \operatorname{cosec}\alpha \log r - 2 \log(\operatorname{cosec}\alpha) + \text{term independent of } \alpha.$$

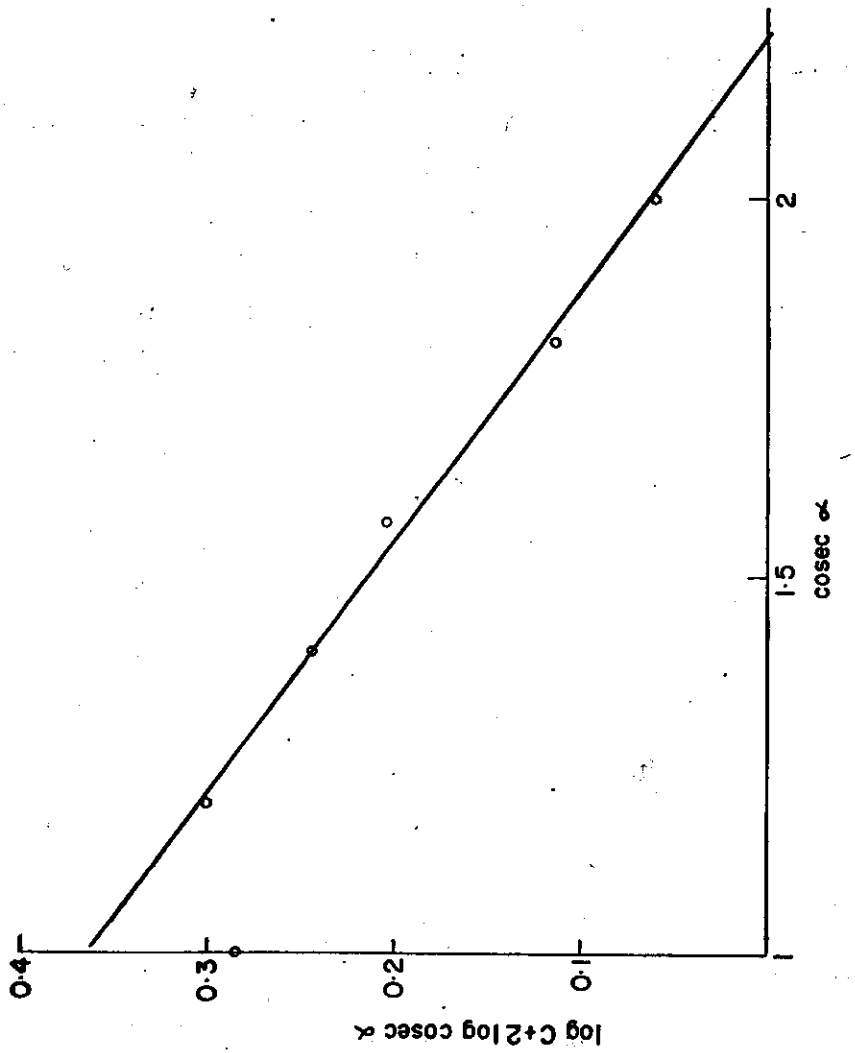
0·4
0·3
0·2
0·1
log C+2 log cosec α
1
1·5
2
cosec α

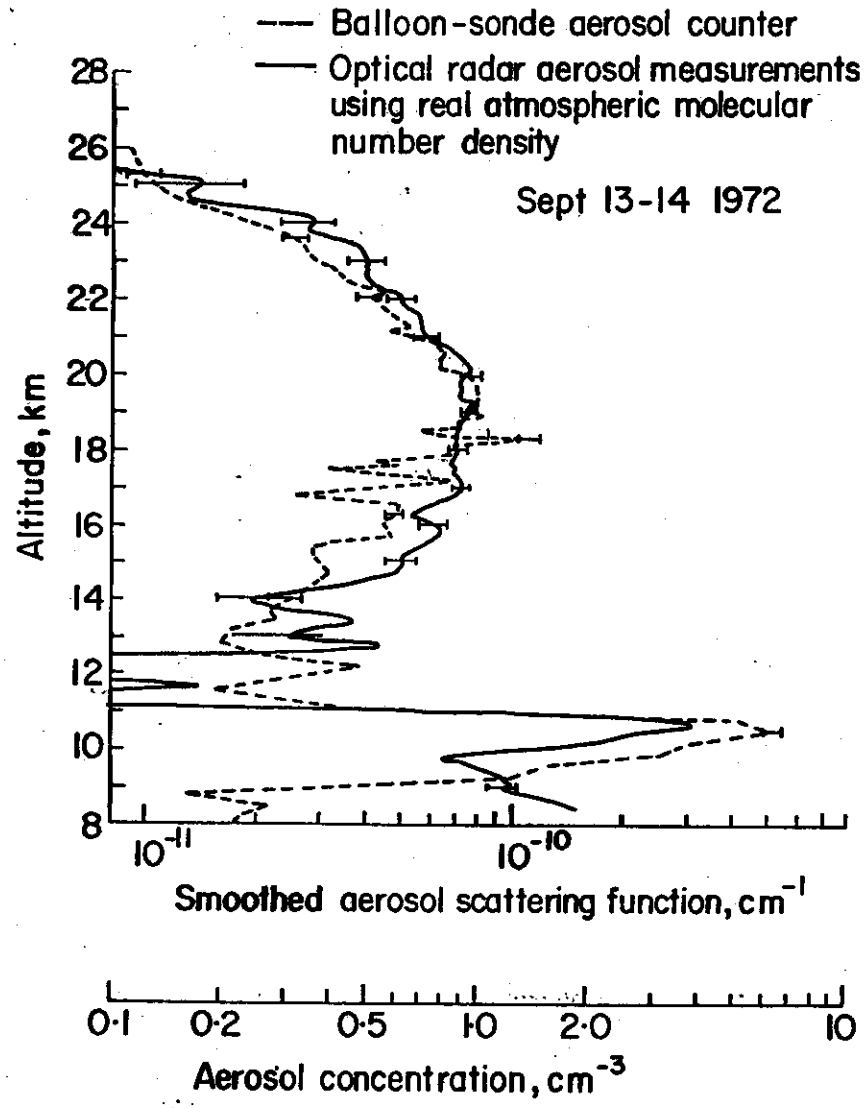
Balloon-sonde aerosol counter
Optical radar aerosol measurements using real atmospheric molecular number density
Sept 13-14 1972
Altitude, km
28
26
24
22
20
18
16
14
12
10
8
10^{-11}
10^{-10}
Smoothed aerosol scattering function, cm^{-1}
0·1
0·2
0·5
1·0
2·0
10
Aerosol concentration, cm^{-3}

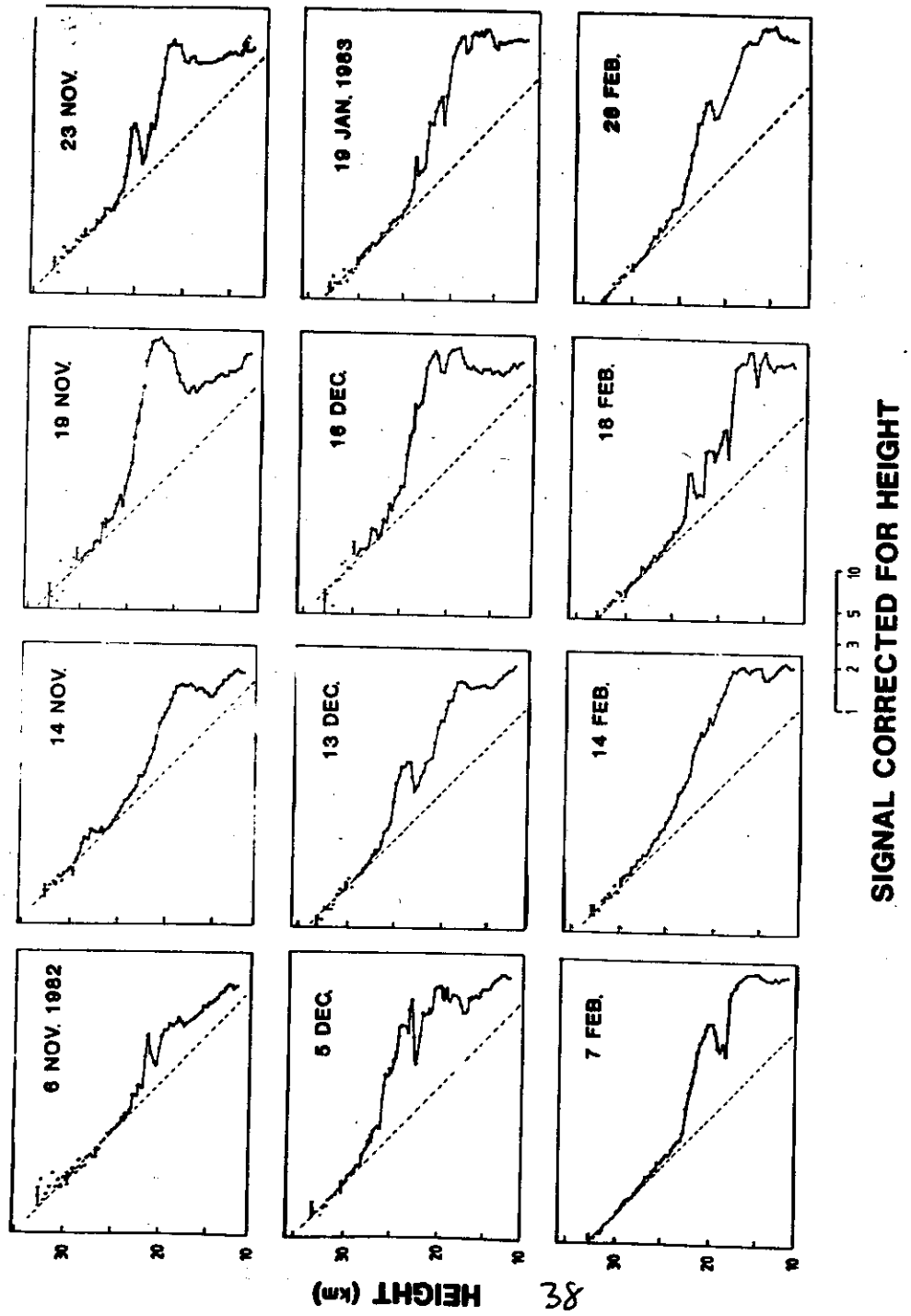
23 NOV.
19 JAN. 1983
28 FEB.
19 NOV.
16 DEC.
18 FEB.
14 NOV.
13 DEC.
14 FEB.
6 NOV. 1982
5 DEC.
7 FEB.
30
20
10
HEIGHT (km)
SIGNAL CORRECTED FOR HEIGHT
1 2 3 5 10

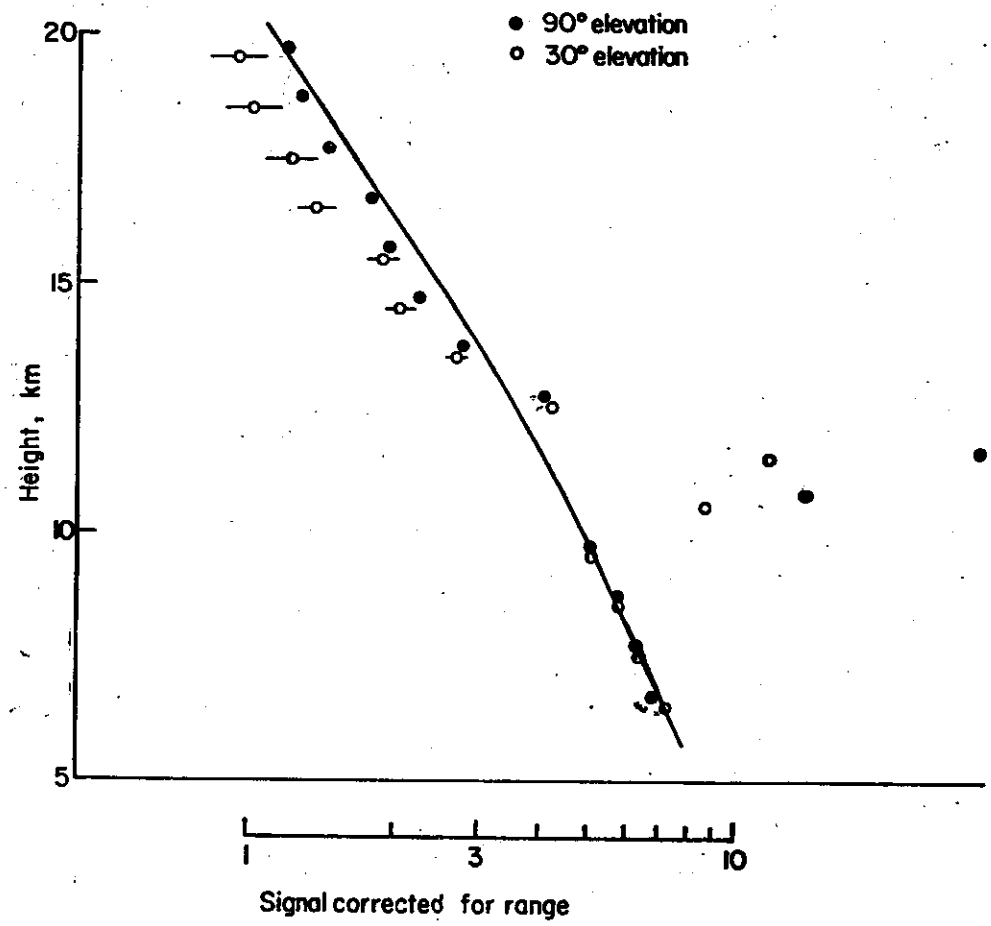
90° elevation
30° elevation
20
15
10
5
Height, km
1
3
10
Signal corrected for range

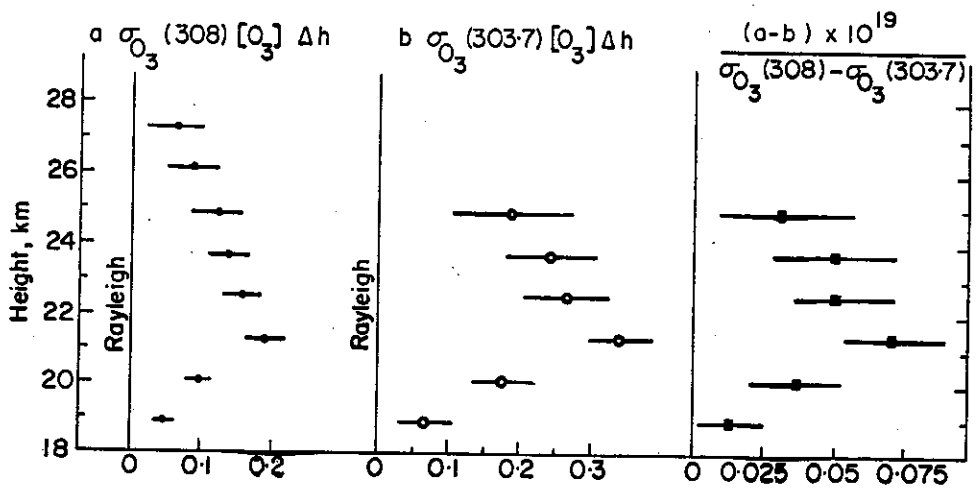
a σ_{O_3} (308) $[O_3]$ Δh
b σ_{O_3} (303·7) $[O_3]$ Δh
$\frac{(a-b) \times 10^{19}}{\sigma_{O_3}(308) - \sigma_{O_3}(303·7)}$
Height, km
Rayleigh
Rayleigh
28
26
24
22
20
18
0 0·1 0·2
0 0·1 0·2 0·3
0 0·025 0·05 0·075

0-4

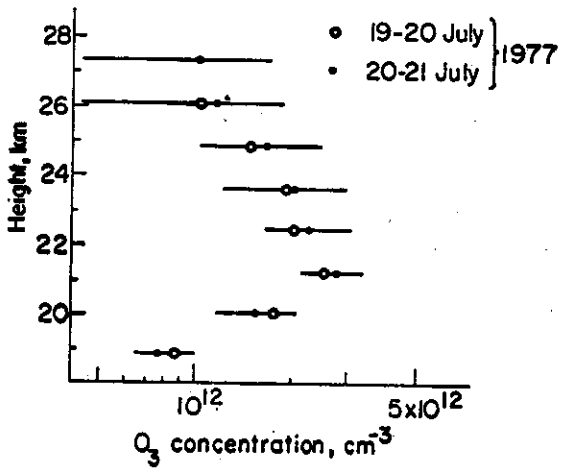
19-20 July
20-21 July
1977
Height, km
28
26
24
22
20
10^{12}
5×10^{12}
O_3 concentration, cm^{-3}

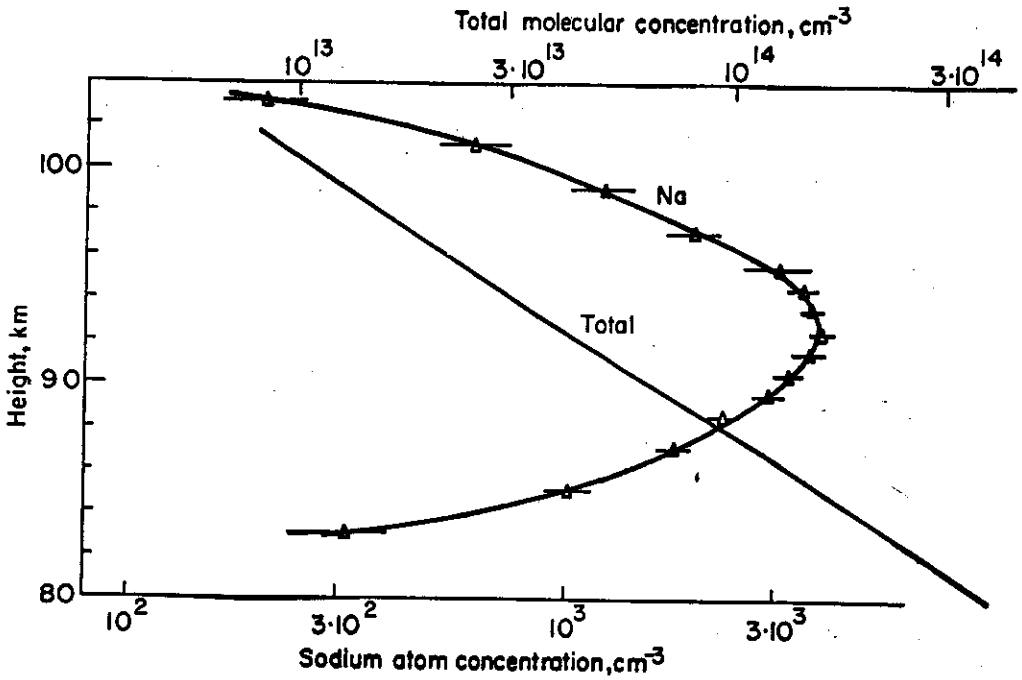
Total molecular concentration, cm^{-3}
10^{13}
$3 \cdot 10^{13}$
10^{14}
$3 \cdot 10^{14}$
Na
Total
Height, km
100
90
80
10^2
$3 \cdot 10^2$
10^3
$3 \cdot 10^3$
Sodium atom concentration, cm^{-3}

1-4

Remote Sensing of Atmosphere

Dobson spectrometer method of observing ozone.

Importance of ozone

1. Shields biological systems from harmful solar UV radiations.
2. Major role in thermal balance of stratosphere, because of its absorption of solar UV radiations and emission of i.r. radiation.
3. Distribution help determine stratospheric heat sources and sinks and therefore controls stratospheric temperature and wind structure.

Both total ozone column content and height distributions are of interest. Dobson method provides the column content and ground-based lidar systems can provide the second.

Dobson method

Provides the longest continuous series of measurements, the method having been used as early as 1925 at some stations.

Method depends on the absorption by ozone of UV radiation from the sun or stars and specifically on the variation of absorption cross section with wavelength in the Huggins bands between 300 and 350 mn.

By Lambert's law, the intensity of radiation at the ground I for radiation of intensity I_o outside the atmosphere is given by

$$I = I_o \exp -[\beta \sec\chi + \delta \sec\chi + \alpha x \sec\chi_h$$

where β = attenuation coefficient for molecular (Rayleigh) scattering

δ = attentuation coefficient for scattering by dust, water droplets etc.

χ = solar zenith angle appropriate to this scattering.

α = ozone absorption coefficient

x = total amount of ozone in a vertical column of cross section 1 cm^2.

χ_h = solar zenith angle near centre of gravity of ozone, and for any value of h can be expressed in terms of X and the radius of Earth.

This expression can be used for two wavelengths, one of which absorbs strongly and the other weakly. All the quantities can be measured or calculated, except x.

In the early application of the method by Dobson (Proc. Phys. Soc. 43, 324, 1931) wavelengths of 311.0 nm and 329.0 nm were used. Recently the use of a double wavelength pair (A - 305.5 nm and 325.4 nm and D - 317.6 nm and 339.8 nm) have been recommended as standard for ozone measurements, i.e. for pair A , $\alpha_A = \alpha_1 - \alpha_2$

pair D , $\alpha_D = \alpha_3 - \alpha_4$

and $\alpha_{AD} = \alpha_A - \alpha_D$

The spectrophotometer makes use of a double dispersing prism P_1 after which the radiation is refocussed on slits S_2S_3. The lens L_2 and prism P_2 recombine the radiation on slit S_5 behind which is a photomultiplier. The measurement approach is then to balance the intensities from S_2 and S_3 using the optical wedges in front of S_3 until the sector wheel which intercepts beams in turn gives rise to no alternating component in the output of the photomultiplier. The positions of the optical wedges then give a direct estimate of the ratio of the two intensities.

The main difficulties arise from

(a) A bias because of errors in the absorption coefficients in the Huggins bands

(b) Variations of the value of I_o, perhaps with solar cycle.

(c) Absorption by other gases, arising out of tropospheric pollution.

A total of 40 currently observing stations have made use of the Dobson method for more than 15 years.

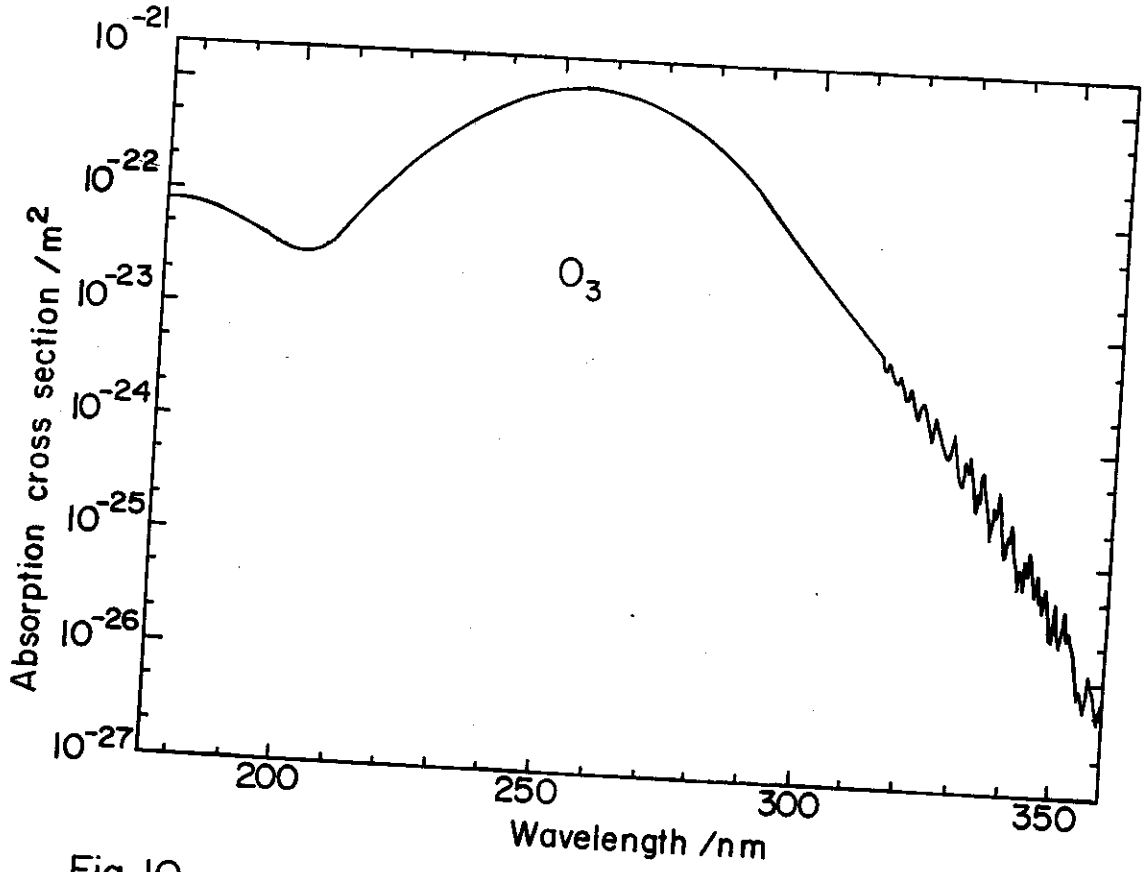

Fig. 10

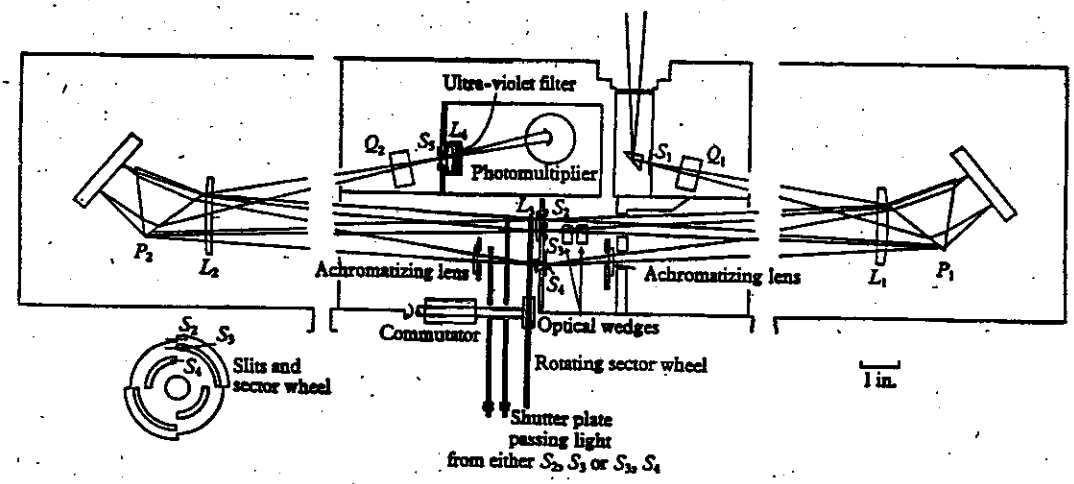

Dobson's ozone spectrophotometer.
(After Normand and Kay, 1952.)

Table 2-1
Dobson Ozone Spectrophotometer Measurement
Error Estimates

Type of Error	Estimated Value*
Systematic Errors	
1. Trend determinations not affected:	
(a) Absorption coefficient uncertainties	(0, +7)%
2. Trend determinations affected (change per decade):	
(a) O_3 absorption coefficient affected by stratospheric temperature changes	± 0.5%
(b) Uncorrected instrument calibration drift	± 3%
(c) Solar spectrum changes	± 0.3%
(d) Aerosol changes	± 1%
** (e) Tropospheric pollution changes with time	
– ozone	± 1%
– other absorbers (e.g., SO_2)	± 2%
(f) Change in cloudiness	± 1%
Random Standard Errors	
3. AD direct sun observations	
– optimal	± 1.5%
– average	± 3%
4. Zenith sky observations	
– optimal	± 2.5%
– average	± 5%

* Using the usual convention ±0.5% means that the % error from this source lies between the limits -0.5 and +0.5, that is, in the interval (-0.5, +0.5)%.
**This is not really an error, but can affect interpretation of stratospheric ozone trends.

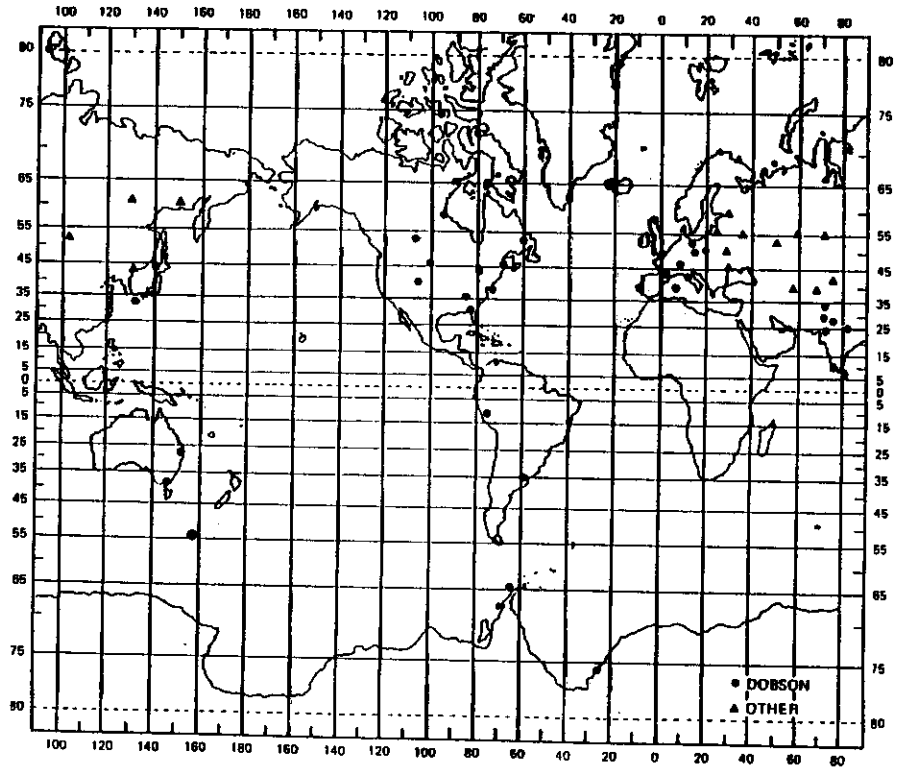

Figure 2-1. Current total ozone observing stations with 15 or more years of observations.